

## ELECTRONIC SUPPORTING INFORMATION

### Development of catalysts for ammonia synthesis based on metal phthalocyanine materials

Natalia Morlanés,<sup>§</sup> Walid Almaksoud,<sup>§</sup> Rohit K. Rai,<sup>§</sup> Samy Ould-Chikh,<sup>§</sup> Mohammed M. Ali,<sup>‡</sup> Balamurugan Vidjayacoumar,<sup>‡</sup> Bedour E. Al-Sabban,<sup>‡</sup> Khalid Albahily,<sup>‡</sup> Jean-Marie Basset<sup>\*§</sup>

<sup>§</sup> KAUST Catalysis Center and Division of Physical Sciences and Engineering, King Abdullah University of Science and Technology (KAUST), Thuwal, 23955-6900, Kingdom of Saudi Arabia.

<sup>‡</sup> SABIC Corporate Research and Development Center at KAUST, Saudi Basic Industries Corporation, Thuwal 23955, Kingdom of Saudi Arabia.

#### Experimental Section

All materials were prepared by pyrolysis of metal phthalocyanines Fe(II)Pc and Co(II)Pc, purchased from Sigma-Aldrich, were used without further purification, following a previously reported procedure.<sup>1</sup> The detailed preparation procedure is the following: A certain amount of precursor, the starting molecule of the metal phthalocyanine, was positioned in a porcelain boat placed in a tubular oven under nitrogen. The temperature was increased to 735 °C (heating rate: 2°C min<sup>-1</sup>) and maintained at that temperature for 6 h. After the pyrolysis the oven cools down to room temperature and the sample is passivated with 1%O<sub>2</sub> in nitrogen for 6 h.

The catalyst FePc + CoPc, was prepared by a physical mixture of Fe(II)Pc and Co(II)Pc (9:1, mass ratio Fe(II)Pc: Co(II)Pc) that was grounded together for 20 minutes in a mortar, before the pyrolysis step described above.

The materials obtained after the pyrolysis of the phthalocyanine precursors, were impregnated with aqueous solutions of cesium nitrate or barium nitrate. The Cs loading (2-10% wt.) and that of Ba (8% wt.).

For the control experiment a sample of Iron supported on carbon was prepared via classical impregnation method; also promoted with cesium (2%Cs-10%Fe/carbon).<sup>2,3</sup> To obtain the carbon support, commercially available activated carbon was heated under inert atmosphere (Nitrogen) at 950°C (heating rate: 5°C min<sup>-1</sup>) for 12 h, followed by cooling to ambient temperature, washing with water to remove the dusty fraction and drying at 100°C overnight. The material thus prepared was impregnated with aqueous solutions of iron nitrate, cobalt nitrate or both (co-impregnation), dried and calcined in air at 220 °C (heating rate: 2°C min<sup>-1</sup>) to convert the salts into their oxides. Then, it was impregnated with aqueous solutions of cesium nitrate to obtain a material with 2% wt. Cs.

#### Characterization of the materials

**Electron Microscopy and Elemental Mapping:** Transmission electron microscopy (TEM) of the samples was performed with a Titan Themis-Z microscope from Thermo-Fisher Scientific by operating it at the accelerating voltage of 300 kV. Prior to the analysis, the microscope was set to scanning TEM (STEM) mode to acquire atomic number (Z) sensitive STEM images with an attached a high-angle annular dark-field (HAADF) detector. Furthermore, a high throughput X-ray energy dispersive spectrometer (EDS) was also utilized in conjunction with DF-STEM imaging to acquire STEM-EDS spectrum-imaging datasets. During the acquisition of these datasets, at every image-pixel, a corresponding EDS spectrum was also obtained for generating

simultaneously the elemental maps of Fe and/or Co C, N, Cs. It is also pertinent to note herein that Spectrum-imaging datasets were acquired in so-called frame mode in which electron beam was allowed to dwell at each pixel for the only time of few microseconds in order to keep a total frame time to merely one second or less. However, each Spectrum-imaging dataset was collected until more than 200 frames were completed. This mode of operation allowed to have a high signal to noise ratio in the acquired STEM-EDS spectrum-imaging datasets while causing a little or no damage to beam-sensitive zeolite samples by the electron beam. Both imaging and spectroscopy datasets for each sample were both acquired as well as analyzed with a newly developed software package called Velox from Thermo Fisher Scientific.

The chemical composition of the catalysts was determined from ICP and elemental analysis using inductively coupled plasma optical emission spectroscopy (ICP–OES) on a Thermo-Electron 3580 instrument.

Powder X-ray diffraction (XRD) measurements were performed on a Bruker D8 Advance reflection diffractometer equipped with a LynxEye energy-discriminating position-sensitive detector (1D-PSD) using Cu K $\alpha$ 1+2 radiation.

Specific surface areas and pore volumes were determined with a Micromeritics ASAP 2010 adsorption analyzer at liquid nitrogen temperature. Before measurements, the materials were degassed at a temperature of 150°C for 10 h. The total pore volume was calculated by using the adsorbed volume at a relative pressure of 0.97. The BET surface area was estimated in the relative pressure range of 0.06–0.2.

### **Metal dispersion and Number of Active surface sites**

The dispersion of iron (FE, mean fraction of the total atoms exposed at the surface) was calculated from the generalized equation<sup>4</sup> and also proposed by Borodzinski and Bonarowska<sup>5</sup> and widely used for iron/carbon catalysts used for ammonia synthesis earlier, using the mean particle size of iron nanoparticles obtained by HR-TEM images considering 120 particles at least. The number of active surface sites was calculated according to the equations provided for iron ammonia synthesis catalysts.<sup>6</sup> The equations are next ones:

$$\text{Dispersion: FE(\%)} = 6 (v_m/a_m)/d$$

$$S_m (\text{m}^{-2} \text{ g}) = 60000 f_m / (\rho \times d)$$

$$\text{NA} (\text{mol g}^{-1}) = f_m \times \text{FE} / M$$

Where:

$a_m$  ( $\text{\AA}^2$ ): The surface area occupied by an atom of metal on a polycrystalline surface. 11.80 and 11  $\text{\AA}^2$  for Fe and Co, respectively.

$v_m$  ( $\text{\AA}^3$ ): The volume occupied by an atom of metal in the bulk of metal; 6.09 and 5.43  $\text{\AA}^3$  for Fe and Co, respectively.

$d$ : mean particle size ( $\text{\AA}$ )

$\rho$ : density of the metal in  $\text{g cm}^{-3}$

$f_m$ : metal loading in the sample, mass fraction wt.

$M$ : molar mass of the metal 55.85 and 58.93 g mol<sup>-1</sup> for Fe and Co, respectively

$D$ : dispersion (FE, mean fraction of the total atoms exposed at the surface)

$S_m$ : Specific metal surface area in m<sup>-2</sup> g

$NA$ : number of active surface sites in mol g<sup>-1</sup>

### **Catalytic activity: Reaction of ammonia synthesis in a continuous flow reactor**

Activity measurements of ammonia synthesis were carried out in a stainless-steel flow reactor supplied with stoichiometric H<sub>2</sub> + N<sub>2</sub> mixture as shown in the **Figure S1**. The flow rate of hydrogen and nitrogen controlled by Brooks mass flow-controllers. The pressure and temperature were kept constant using the correspondent controllers. In general, 200 mg of catalyst and a total flow of 40 ml min<sup>-1</sup> are used for the experiments, keeping H<sub>2</sub>:N<sub>2</sub> ratio 3:1. The reactor outlet is connected to the Mass-Vac Spectrometer for continuous monitoring of the NH<sub>3</sub> mass signal (Mass = 17). Ar (0.6 ml min<sup>-1</sup>) is used as reference for the calibration of the instrument (see below).

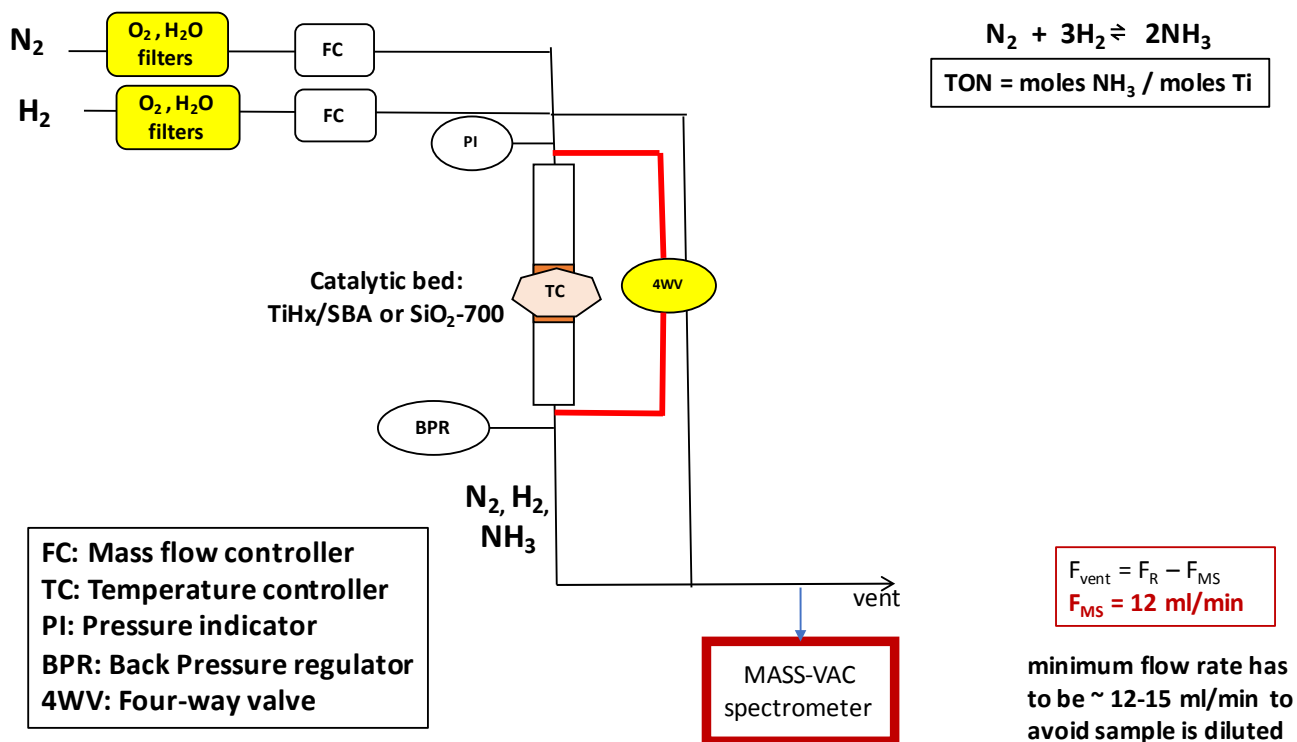


**Figure S1.** Experimental Setup with mass spectrometer connected online.

Prior to measurements, the samples were reduced in a H<sub>2</sub>:N<sub>2</sub> stream with a total flow of 40 ml min<sup>-1</sup>, at 485 °C for 36 h (Cesium- promoted iron catalysts) and at 520°C for 48 h (Barium-promoted cobalt catalyst) (heating rate 4°C min<sup>-1</sup>); according to previously reported procedures. Activation at higher temperature than those indicated resulted in a decrease of the catalytic performance for the iron-based catalysts. The signal of ammonia was monitored during the activation pre-treatment until this signal was constant, after that the catalysts are considered under the steady-state conditions.

The commercial Iron-benchmark KM-1 catalyst was activated under  $H_2/N_2$  atmosphere (3/1 molar ratio) following the reported procedure;<sup>7</sup> a two-step reduction process using a slow linear heating ramp ( $4^\circ C / min$ ) from 25 to  $525^\circ C$  for 40 h, with an isothermal break of several hours (6h) at the point of maximum water evolution ( $225^\circ C$ ).

The reaction temperature was varied in the range  $400-550^\circ C$ , and the pressure from atmospheric to 70 bar. During the experiments, each set of conditions was kept constant for 1 h to ensure a stable performance was reached and to analyze the ammonia in the reactor outlet using the online connected Mass-Vac Spectrometer. From the concentration of ammonia in the outlet gas, the reaction rate was determined and expressed in  $NH_3 \mu mol g^{-1} h^{-1}$ .

The ammonia signal monitored by the mass-Vac is converted into the concentration of ammonia in the outlet gas by the calibration curve previously obtained for the instrument, using Ar inert gas as reference. The calibration curve (**Figure S2**) was obtained for gas mixtures of known concentration of ammonia in  $N_2:H_2$  (3:1) mixtures. And the calculation procedure in order to convert the signal monitored in the mass spectrometer to the moles of  $NH_3$  and to the ammonia synthesis rate, is described here:

- 1) The signal for the ammonia in Torr is converted into ppm of  $NH_3$  using the calibration curve (Figure S2)
- 2) Then ppm of ammonia is converted into flow rates in ml/min and mol/min using next equations:
- 3)  $ml NH_3 (NTP)/min = ppm NH_3 \times 1.10^{-6} \times total\ flow\ rate\ (ml/min)$
- 4)  $moles\ NH_3/min = (ml\ NH_3\ (NTP)/min / 1000ml) \times 1\ atm / [0.082\ atm\ L/mol/K \times 293.15\ K]$
- 5)  $NH_3\ rate\ (\mu mol\ g^{-1}\ h^{-1}) = (moles\ NH_3/min \times 60\ min/h \times 1.10^6\ \mu mol/mol) / mass\ catalyst\ (g)$

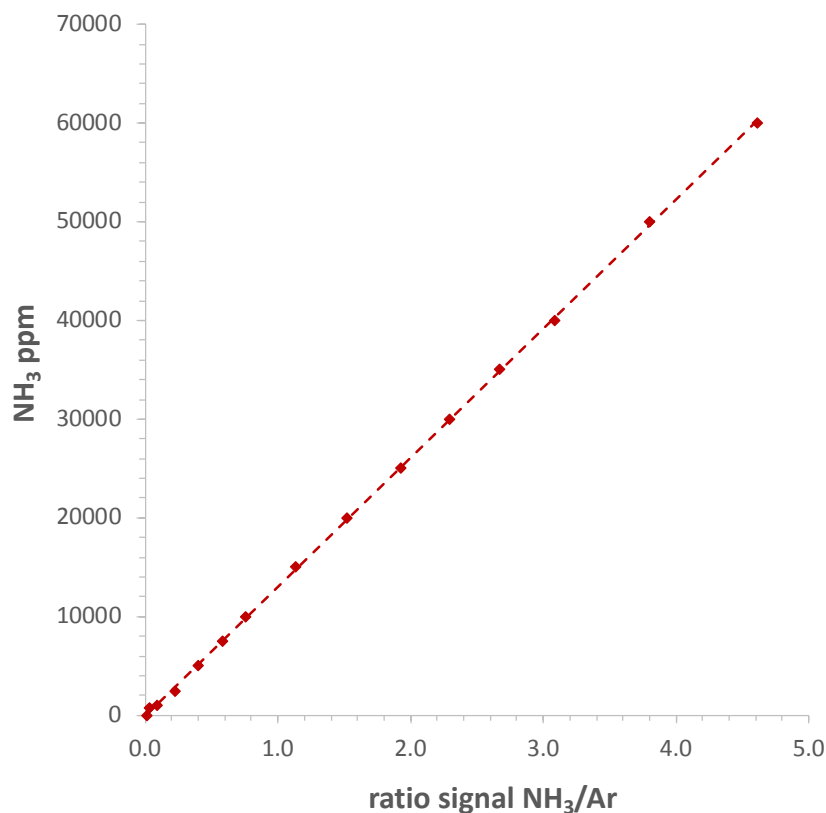


**Figure S2.** Calibration curve to convert the signal of ammonia monitored in the Mass-Vac Spectrometer into NH<sub>3</sub> concentration in the reactor outlet.

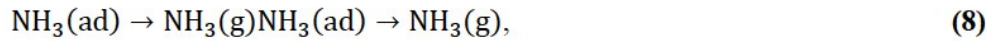
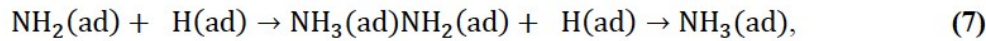
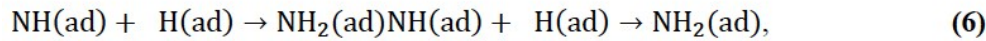
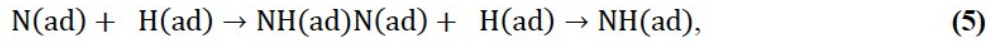
The activity evaluated per the number of active surface sites (N.A) is reported as the turnover frequency. It is calculated according the next equation:

$$\text{TOF (s}^{-1}\text{)} = \text{NH}_3 \text{ rate } (\mu\text{mol g}^{-1} \text{ h}^{-1}) \times 1.10^{-6} (\mu\text{mol/mol}) / \text{NA (mol g}^{-1}\text{)}/3600 (\text{s h}^{-1})$$

The N<sub>2</sub> and H<sub>2</sub> reaction orders measurement were carried out with a total flow rate of 60 ml min<sup>-1</sup> of mixed gas (N<sub>2</sub>, H<sub>2</sub>, Ar), at constant total pressure (10 bar) and temperature (400°C). For the N<sub>2</sub> order measurement the H<sub>2</sub> flow rate was 45 ml min<sup>-1</sup> kept constant, and the flow rate of N<sub>2</sub> is changing while keeping (N<sub>2</sub> +Ar) in 15 ml min<sup>-1</sup>. For the H<sub>2</sub> order measurement the N<sub>2</sub> flow rate was 15 ml min<sup>-1</sup> kept constant, and the flow rate of H<sub>2</sub> is changing while keeping (H<sub>2</sub> +Ar) in 55 ml min<sup>-1</sup>. The reaction order with respect to NH<sub>3</sub> was obtained by changing the flow rate of syngas in the range 40-120 ml min<sup>-1</sup>, while keeping a constant N<sub>2</sub> and H<sub>2</sub> partial pressure (H<sub>2</sub>:N<sub>2</sub> ratio 3:1).<sup>8</sup> All the kinetic measurements were conducted under conditions far from equilibrium.

### **Kinetic calculations**

The rate-determining step (RDS) for ammonia synthesis was examined by fitting the modeled rate equations to a set of obtained reaction rates. The rate equations were expressed by the Langmuir–Hinshelwood mechanism.<sup>9,10,11,12,13</sup> The following sequence of elementary steps can be expressed for the overall reaction:



where (g) and (ad) denote gas-phase and adsorption species, respectively. Among these steps, steps (4)–(7) control the overall rate of reaction due to the large activation energy. The partial pressure of  $\text{NH}_3$  ( $P_{\text{NH}_3}$ ) was omitted when it was sufficiently small compared with  $P_{\text{N}_2}$  and  $P_{\text{H}_2}$  at the outlet. Under the reaction conditions employed,  $P_{\text{NH}_3}$  of the obtained experimental rates were much smaller than  $P_{\text{N}_2}$  and  $P_{\text{H}_2}$  at the outlet, and the equilibrium value, which reasonably satisfied the applicable condition of the calculated equations derived with elimination of the  $P_{\text{NH}_3}$  term and the reverse reaction. The final rate equations are as follows<sup>5,6,7,8,9</sup>:

$$r = \frac{\overrightarrow{k}_4 K_2 P_{\text{N}_2}}{(1 + K_1 P_{\text{H}_2} + K_2 P_{\text{N}_2} + \sqrt{K_1 K_3 P_{\text{H}_2}})^2}, \quad (9)$$

$$r = \frac{\overrightarrow{k}_5 \sqrt{K_1 K_2 K_3 K_4} \sqrt{P_{\text{H}_2} P_{\text{N}_2}}}{(1 + K_1 P_{\text{H}_2} + K_2 P_{\text{N}_2} + \sqrt{K_1 K_3 P_{\text{H}_2}} + \sqrt{K_2 K_4 P_{\text{N}_2}})^2}, \quad (10)$$

$$r = \frac{\overrightarrow{k}_6 K_1 K_3 K_5 \sqrt{K_2 K_4} \sqrt{P_{\text{H}_2} P_{\text{N}_2}}}{(1 + K_1 P_{\text{H}_2} + K_2 P_{\text{N}_2} + \sqrt{K_1 K_3 P_{\text{H}_2}} + \sqrt{K_2 K_4 P_{\text{N}_2}} + K_5 \sqrt{K_1 K_2 K_3 K_4 P_{\text{H}_2} P_{\text{N}_2}})^2}, \quad (11)$$

$r =$

$$\frac{\overrightarrow{k}_7 K_1 K_3 K_5 K_6 \sqrt{K_1 K_2 K_3 K_4} \sqrt{P_{\text{H}_2} P_{\text{N}_2}}}{(1 + K_1 P_{\text{H}_2} + K_2 P_{\text{N}_2} + \sqrt{K_1 K_3 P_{\text{H}_2}} + \sqrt{K_2 K_4 P_{\text{N}_2}} + K_5 \sqrt{K_1 K_2 K_3 K_4 P_{\text{H}_2} P_{\text{N}_2}} + K_1 K_3 K_5 K_6 \sqrt{K_2 K_4 P_{\text{N}_2} P_{\text{H}_2}})^2}, \quad (12)$$

where  $k_4$ ,  $k_5$ ,  $k_6$ ,  $k_7$ , are the rate constant of the forward reactions 4-7, and  $K_i$  is the equilibrium constant in step  $i$ . Equations (9)-(12) are expressed based on the assumption that steps (4)-(7) are the RDS, respectively. In order to examine the RDS for ammonia synthesis, the derived

equations were separately fitted into sets of experimental rates using a least squares method and evaluated to determine which equations best described the experimental rates.

**Other data**

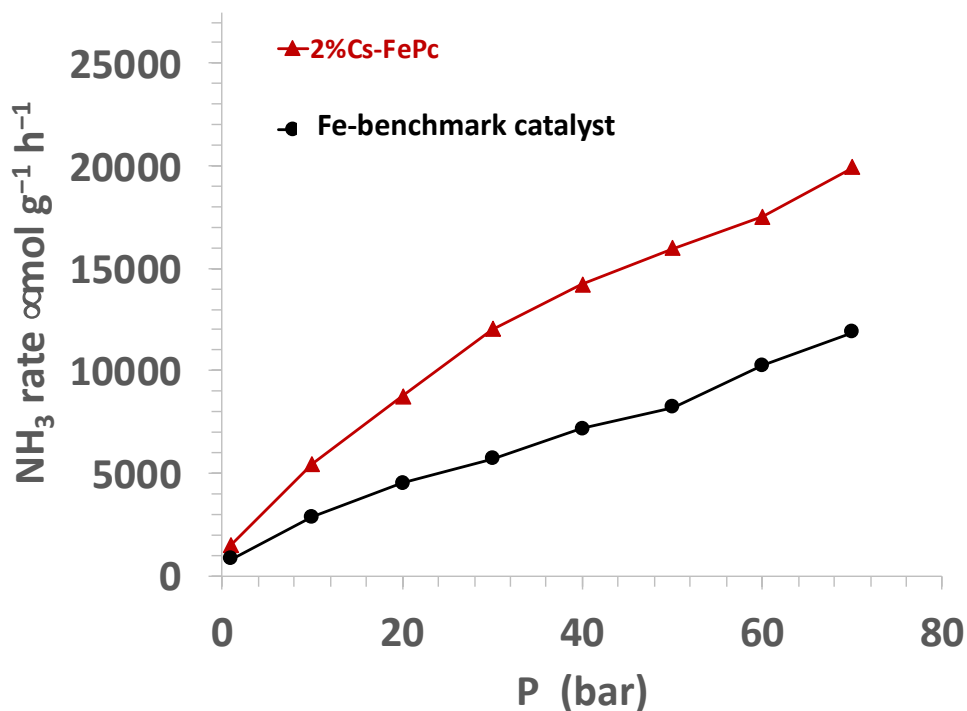


**Figure S3.** Catalytic performance of the 2%Cs-FePc catalysts for the ammonia synthesis reaction. NH<sub>3</sub>-synthesis rate as a function of the pressure at 400 °C. Reaction conditions: 200 mg of catalyst, flow rate 40 ml min<sup>-1</sup>, N<sub>2</sub>:H<sub>2</sub> = 1:3, with a WHSV of 12000 ml g<sup>-1</sup> h<sup>-1</sup>, P = 1-70 bar, T = 400 °C

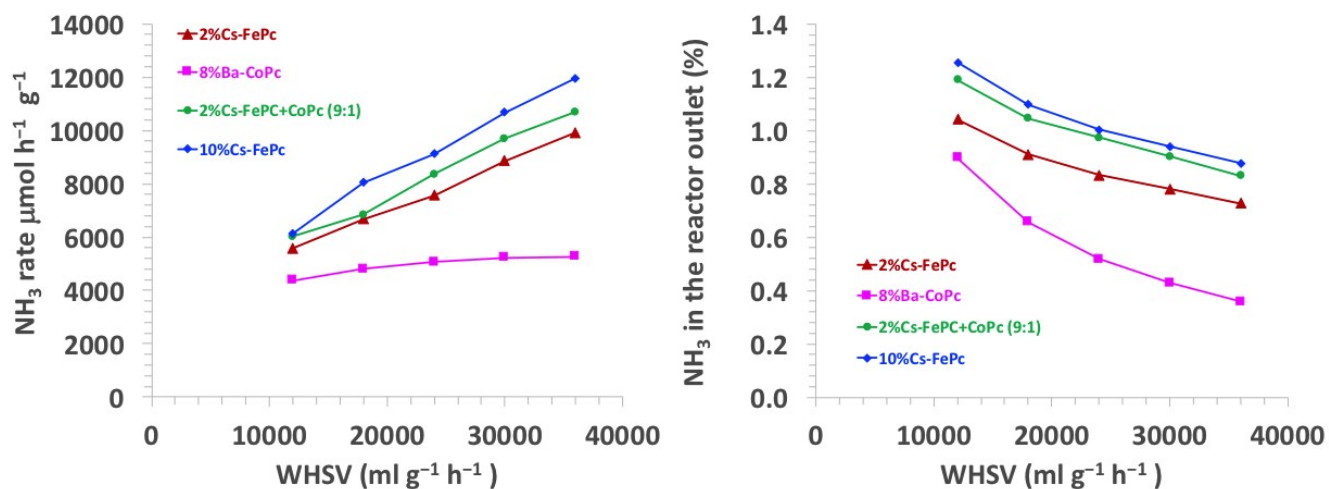


**Figure S4.** Catalytic performance phthalocyanine derived catalysts for the ammonia synthesis reaction. Influence of the space velocity at 10 bar and 400 °C. Reaction conditions: 200 mg of catalyst, flow rate 40-120 ml min<sup>-1</sup>, N<sub>2</sub>:H<sub>2</sub> = 1:3, with a WHSV of 12000-40000 ml g<sup>-1</sup> h<sup>-1</sup>, P = 10 bar, T = 400 °C

**Table S1.** Kinetic parameters of selected catalysts from literature

Catalyst	E <sub>a</sub> (kJ mol <sup>-1</sup> )	N <sub>2</sub> order (α)	H <sub>2</sub> order (β)	NH <sub>3</sub> order (γ)	Ref
Fe-benchmark	70	0.9	2.2	-1.5	<sup>14, 15</sup>
Co <sub>3</sub> Mo <sub>3</sub> N	55.6	0.99	0.8	-1.34	4
2%Cs-Co <sub>3</sub> Mo <sub>3</sub> N	56.8	0.96	0.89	-0.89	4
8%Ba-10%Co/carbon	103	0.9	1.5	-1.1	11
LaCoSi	42	0.45	0.8	-1.5	5
Fe-LiH	46.5	0.37	0.88	-1.3	<sup>16</sup>
Co-LiH	52.1	0.48	0.65	-1.2	12
Ru/C12A7:e	49	0.46	0.97	-1.0	<sup>17</sup>
Cs-Ru/MgO	106	1.0	-0.43	-0.12	<sup>18</sup>

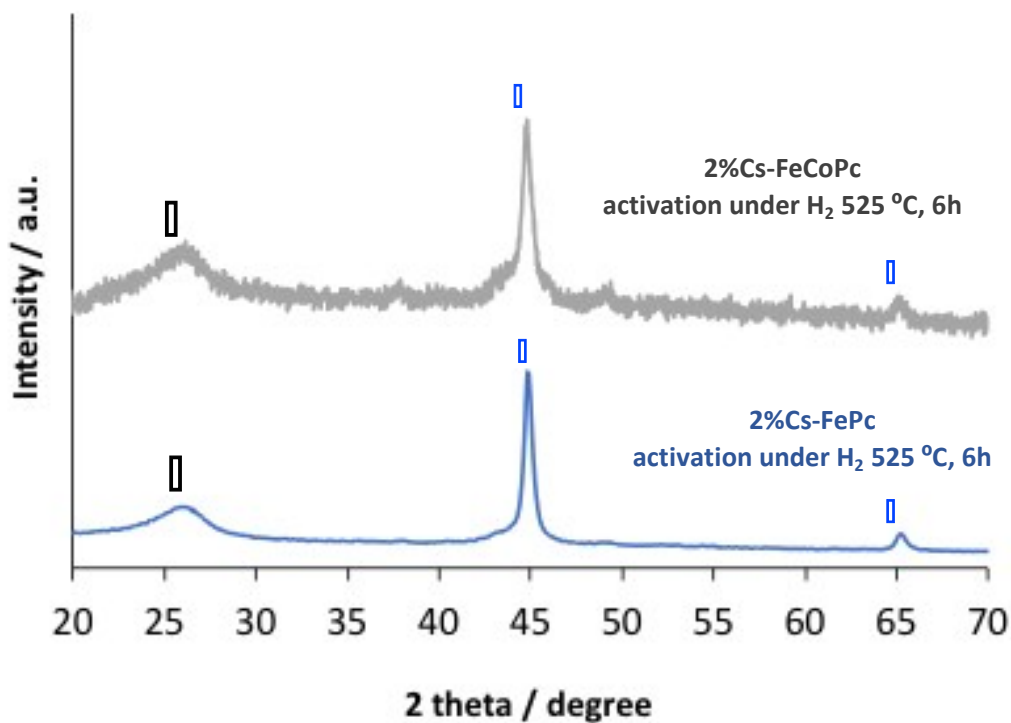


**Figure S5.** XRD Patterns 2%Cs-FePc and 2%Cs-FeCoPc catalysts, after activation under hydrogen. Fe (★), Fe<sub>3</sub>C(◆)  
Carbon (◇).

## REFERENCES

---

- <sup>1</sup> Harun Tuysuz, Ferdi Schuth, Linjie Zhi, Klaus Mullen, Massimiliano Comotti, "Ammonia Decomposition over Iron Phthalocyanine-Based Materials" *ChemCatChem* 2015, 7, 1453 – 1459
- <sup>2</sup> W. Rarog-Pilecka, A. Jedynak-Koczuk, J. Petryk, E. Miskiewicz, S. Jodzis, Z. Kaszkur, Z. Kowalczyk, "Carbon-supported cobalt–iron catalysts for ammonia synthesis" *Applied Catalysis A: General* 300 (2006) 181–185
- <sup>3</sup> Anna Jedymak, Dariusz Szmigiel, Wioleta Rarog, Jerzy Zielinski, Jerzy Pielaszek, Piotr Dluzewski, Zbigniew Kowalczyk, "Potassium promoted carbon-based iron catalyst for ammonia synthesis. Effect of Fe dispersion, *Catalysis Letters*, 81 (2002) 213-218
- <sup>4</sup> Bergeret, G. and Gallezot, P. (2008). Particle Size and Dispersion Measurements. In *Handbook of Heterogeneous Catalysis* (eds G. Ertl, H. Knözinger, F. Schüth and J. Weitkamp
- <sup>5</sup> Borodzinski and Bonarowska, *Langmuir* 13(21) 1997, 5613
- <sup>6</sup> Huazhang Liu, Wenfeng Han, *Catalysis Today* 297 (2017) 276–291
- <sup>7</sup> R. Schlogl, "Catalytic Ammonia Synthesis" J. R. Jennings ed., Plenum Press, New York, 19-108 (1991)
- <sup>8</sup> Ryoichi Kojima, Ken-ichi Aika, "Cobalt molybdenum bimetallic nitride catalysts for ammonia synthesis Part 2. Kinetic study" *Applied Catalysis A: General* 218 (2001) 121–128
- <sup>9</sup> Yutong Gong, Jiazhen Wu, Masaaki Kitano, Junjie Wang, Tian-Nan Ye, Jiang Li, Yasukazu Kobayashi, Kazuhisa Kishida, Hitoshi Abe, Yasuhiro Niwa, Hongsheng Yang, Tomofumi Tada, Hideo Hosono, "Ternary intermetallic LaCoSi as a catalyst for N<sub>2</sub> Activation, *Nature Catalysis*, 2018, <https://doi.org/10.1038/s41929-017-0022-0>
- <sup>10</sup> Masaaki Kitano, Yasunori Inoue, Masato Sasase, Kazuhisa Kishida, Yasukazu Kobayashi, Kohei Nishiyama, Tomofumi Tada, Shigeki Kawamura, Toshiharu Yokoyama, Michikazu Hara, Hideo Hosono, "Self-organized Ruthenium–Barium Core–Shell Nanoparticles on a Mesoporous Calcium Amide Matrix for Efficient Low-Temperature Ammonia Synthesis", *Angew. Chem. Int. Ed.* 2018, 57, 1 – 6
- <sup>11</sup> Y. Kobayashi, M. Kitano, S. Kawamura, T. Yokoyama, H. Hosono, "Kinetic evidence: the rate-determining step for ammonia synthesis over electronegative supported Ru catalysts is no longer the nitrogen dissociation step", *Catal. Sci. Technol.* 2017, 7, 47 – 50
- <sup>12</sup> Siporin, S. E., Davis, R. J., "Use of kinetic models to explore the role of base promoters on Ru/MgO ammonia synthesis catalysts", *J. Catal.* 225, 359–368 (2004).
- <sup>13</sup> K. Aika, M. Kumasaka, T. Oma, O. Kato, H. Matsuda, N. Watanabe, K. Yamazaki, A. Ozaki, T. Onishi, *Appl. Catal.* 28 (1986) 57
- <sup>14</sup> Jens Sehested, Claus J. H. Jacobsen, Eric Tornqvist, Said Rokni, Per Stoltze, "Ammonia Synthesis over a Multipromoted Iron Catalyst: Extended Set of Activity Measurements, Microkinetic Model, and Hydrogen Inhibition", *Journal of Catalysis* 188 (1999) 83–89
- <sup>15</sup> Stefan Hagen, Rasmus Barfod, Rasmus Fehrmann, Claus J. H. Jacobsen, Herman T., Teunissen, Kenny Ståhlb and Ib Chorkendorff, "New efficient catalyst for ammonia synthesis: barium-promoted cobalt on carbon", *Chem. Commun.*, 2002, 1206–1207
- <sup>16</sup> Peikun Wang, Fei Chang, Wenbo Gao, Jianping Guo, Guotao Wu, Teng He, Ping Chen, "Breaking scaling relations to achieve low-temperature ammonia synthesis through LiH-mediated nitrogen transfer and hydrogenation" *NATURE CHEMISTRY*, 9 (2017) 64-70
- <sup>17</sup> Kitano, M. et al. Ammonia synthesis using a stable electronegative as an electron donor and reversible hydrogen store. *Nat. Chem.* 4, 934-940 (2012)
- <sup>18</sup> Hagen, S. et al. Ammonia synthesis with barium-promoted iron-cobalt alloys supported on carbon. *J. Catal.* 214, 327-335 (2003)